Power Sharing Based Control Strategy for a 350 kW Multiport EV Charging System

Abhijit Choudhury, Yuichi Mabuchi, and Kimihisha Furukawa
Hitachi Ltd., Research and Development Group
Hitachi-shi, Ibaraki-ken, Japan
abhijit.choudhury.uz@hitachi.com

Abstract—**Due to the immerging market for the ultrafast EV charging solutions to cater the need for EV chargers, multiport charging solutions are nowadays very popular. To reduce the overall footprint size of converter, solid state transformer (SST) based power converter is a preferred choice. The conventional EV chargers can either charge high power EVs or can charge multiple smaller power EVs with the help of multiple DC/DC converters. So, in this research work a 6.6 kV SST based charging solution is proposed, which can charge both the high (350 kW) and low power EVs (50 kW x 7) simultaneously. In the proposed system, the common LV DC-bus can directly charge a high-power EV and it is also shared with other lower power EVs through additional DC/DC converters. The common DC-bus can also be charged from one of the connected EV batteries and it can be shared with other EVs, in case there is a grid failure. Detailed simulation studies are performed to demonstrate the system performance. One of the SST cell unit is also manufactured, and experimental tests are performed to verify the system operation.**

Keywords—MSC, fast charger, DC bus voltage balancing, cell power balancing.

I. INTRODUCTION

High power modular converters are becoming more and more popular due to their rapid growth in the renewable energy and transportation sector. For transportation sector ultrafast chargers are more popular due to their quick charging capability (< 10 minutes) at a high-power level [1]. For such applications if the space and modularity is a main point of concern, then the high frequency modular type converters such as MSC (Multistage converter) or MMC (Modular multilevel converter) could be a preferred choice. For our application MSC type of converter is considered due to their comparatively lower cost as compared to the MMC type, for 6.6 kV and 350 kW application.

Reference [2] discussed about a DC bus voltage balancing scheme for a series connected units for single phase application. The proposed scheme helps to keep the DC bus voltage stable and feeds power back to the grid side. The decoupled control helps to separately controls the DC bus voltages.

A small signal model-based control for MSC type converter is proposed in reference [3]. There are in total five series connected units. The proposed system uses a common DC bus configuration, which connects all the AC/DC/DC converter outputs together. Detailed simulation and experimental results are performed to show the effectiveness of the proposed control system.

A PI based control strategy to control the DC bus voltages of a series connected H-bridge active rectifier is proposed in [4]. The proposed strategy helps to keep the DC bus voltages at the desired level for all the rectifiers separately. The proposed control strategy is then verified by simulation and experimental results for the two series connected cell units.

Power flow study of a multiport SST network is presented in ref. [5]. The proposed study helps to demonstrate the flexibility of such kind of converter while controlling bi-directional power flow.

A DC-bus voltage balancing strategy for a 7.2 kV system is proposed in [6]. The proposed system uses three cell units and output from all the cell units are connected together to form a common DC bus. The common DC-bus voltage output is then feedback to the grid with the help of an additional three phase DC/AC converter. The proposed control uses a 3D space modulation technique. The proposed technique helps to select the most appropriate vector which balances the DC link capacitor voltages quickly, keeps the system stable with resistive, inductive and capacitor loads as well.

Ref. [7] shows a SST based 400 kW charger with a common LV DC bus configuration with 13.2 kV grid side voltage. The proposed system generates a common LV DC-bus voltage of 1.05 kV. It is then shared with multiple buck converters to provide a charging voltage of 200 - 1000 V to the connected EVs. The proposed system can charge only one EV at a time, which is not preferable for a large-scale EV charging solution.

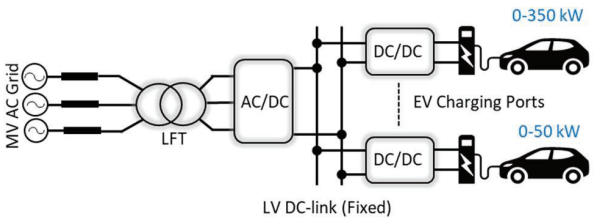

Fig. 1. Conventional LFT (Low frequency transformer) based multiport EV charging solution.

In ref. [8] a multiterminal SST based EV charging solution is proposed. In this configuration several DC/DC converters are connected in parallel to serve multiple EVs simultaneously. An energy storage device like battery is also connected at the LV DC-bus to store energy and deliver it to the chargers based on their requirements.

Ref. [9] proposed a multi winding transformer-based EV charging solution with a third winding. The output of multi winding transformer is connected to multiple EVs and the third winding shares the zero-sequence current between the three phases. Here, the charging power of all the EV charging ports are similar.

In a different configuration of SST shown in ref. [10], electrolytic capacitors are removed, and the front-end AC/DC converter is replaced by an uncontrolled diode rectifier. The secondary side converter is also replaced by a diode rectifier.

An overall system loss reduction strategy is proposed in ref. [11] with a faster DC charging capacity for a single phase SST application. Detailed simulation results are presented to show the loss distribution and system overall response.

In ref. [12] a multiport 350 kW EV charging solution is proposed, where multiple EVs can be charged simultaneously at a different charging rates based on the requirement. Detailed simulation studies are performed to demonstrate the performance of the system with multiple EVs simultaneously. HIL based simulation is also shown to demonstrate the results.

All the converter topologies discussed in the references are based on the common LV DC bus configuration. These topologies either charges a high-power EV directly or it charges multiple lower power EVs simultaneously, through DC/DC converters. In the proposed system, a common DC-bus configuration is developed, which can charge both the high and lower power EVs simultaneously. The proposed converter configuration can even charge or discharge EVs which are connected to the same bus bar when AC grid voltage is not available. Detailed simulation and experimental results are shown in the following sections.

II. CONVENTIONAL LFT AND SST CONVERTER BASED EV CHARGING SOLUTION

Fig. 1 shows one of the schematic configurations of the conventional multiport EV charging solutions. In this system a LFT steps down the MVAC voltage (6.6 kV) to LV AC (400 V) level. An active front end converter is then used to convert the AC voltage to DC, which is then shared with other multiple DC/DC converters for EV charging. Although, it is a very simple, convenient, and widely used solution to charge EVs, it consumes a lot of space and weight is also high. Hence, to overcome this issue a SST based solution is proposed in Fig. 2.

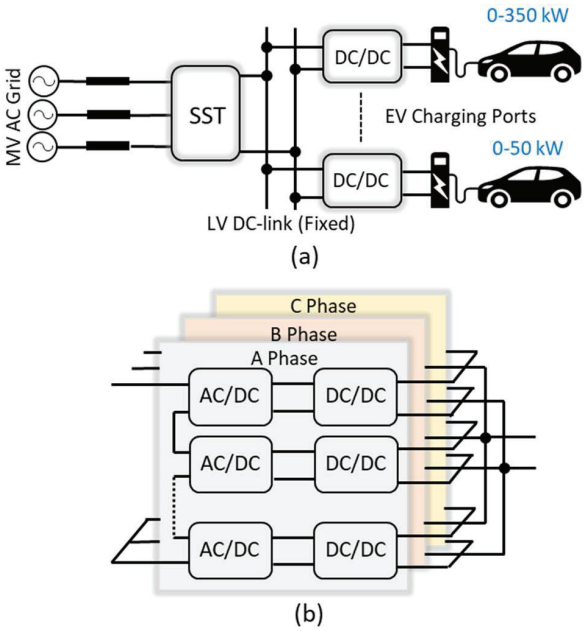

Fig. 2. Conventional SST converter-based multiport EV charging solution, (a) Converter overall schematic; (b) SST converter internal cell configuration.

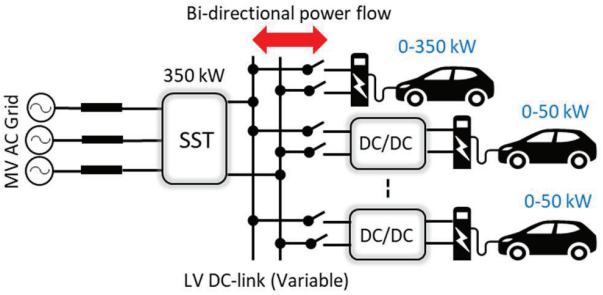

Fig. 3. Proposed SST based multiport EV charging solution.

In this configuration, the input side of the converter is directly connected to the MVAC grid without any LFT, which saves overall system space requirement and weight. The converter is consisting of multiple series connected cell units and each cell is consisting of cascaded AC/DC and DC/DC converters. The AC/DC converter is a conventional H-bridge type, and the DC/DC converter could be a bidirectional or unidirectional DAB, LLC or CLLC type. LLC converters are preferable than the DAB type, due to their lower converter loss for fixed output voltage application.

The output terminal is then forms a common LV DC-bus, which is then shared with multiple DC/DC converters to charge EVs. Some energy storage devices can also be connected at the common LV DC-bus, to store energy or integrate with other renewable energy sources.

III. PROPOSED SST CONVERTER BASED EV CHARGING SOLUTION

One of the issues with the conventional system shown in Fig. 2 is that for high power charging, a separate high-power DC/DC converter is required. This will add additional cost to the system. Alternatively, an external array of switches needs to be used to club all DC/DC converter outputs together to feed one single EV. This will also increase the space requirement and complexity to the system.

To overcome from this issue, a direct integration of an high power EV charging port at the SST output (LV DC Bus) is proposed, as shown in Fig. 3. The LV DC bus is also then shared with other DC/DC converters, which can charge the remaining lower power EVs (0-50 kW) respectively. As compared to the conventional charging solution, in the proposed configuration, the LV DC bus voltage is variable. The system controller will vary the LV DC-bus voltage to meet the requirement for the directly connected high power EV charger. The remaining available power will be then feed to other connected EVs through the connected DC-DC converters. The DC/DC converters will change the phase shift angle to meet the input voltage variation. Table I shows the comparison study between the conventional and the proposed system. As mentioned earlier, the proposed system will have a much lower footprint size and cost due to the reduction of additional high-power DC/DC converter. However, control complexity would be little higher.

Table I : Overall System Comparison (H: High; M: Moderate; L: Low)

System Type	Footprint Size	Cost	Control Complexity
Conventional	H	M	M
Proposed	L	L	M

In Fig. 4 three different modes of operations are shown for the proposed configuration.

a. Mode I: In this mode of operation, SST distributes the available power to all the EVs based on their requirements. Initially controller checks for charging power required by each charging port and initially meets the requirement for the high-power charging port. The remaining power is then distributed to the other EVs based on their requirements. The LV DC-bus voltage will vary based on the EV1 charging power requirement and it will set the LV DC-bus voltage reference for the other connected EVs.

ii. Mode II: In this mode of operation, the MV grid voltage is disconnected from the SST. So, there is no grid power available to charge the connected EVs. In such condition, the connected bi-directional DC/DC converters can charge/discharge each other based on the available EV battery power and the charging power requirements.

iii. Mode III: The connected EVs can also feed power back to the grid as well to support the grid, if there is any such requirement (V2G operation).

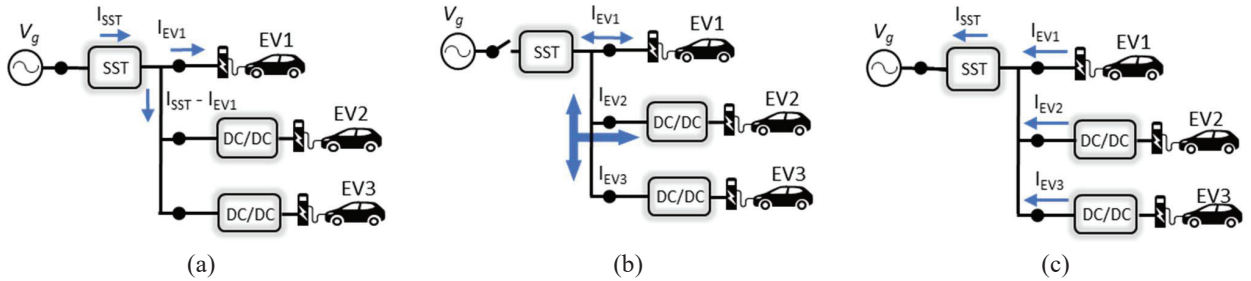

Fig. 4. Proposed charger different modes of operations; (a) Mode I; (b) Mode II; (c) Mode III.

IV. PROPOSED CONTROL STRATEGY

Fig. 4 shows the control circuit configuration to keep all the cell voltages stable. Although, outputs from all the cell converters are connected together to form a common DC-bus and all cell units will feed the same power, there might still be an power imbalance in between the cell units due to the component nonlinearities. PLL shown in Fig. 5 (a) generates the grid reference voltage phase angle (θ_g), which is in synch with the grid voltage. The grid angle is then used to convert the three phase grid voltages ($v_{ag,bg,cg}$) and currents ($i_{ag,bg,cg}$) to d,q frame ($v_{d,q}$, $i_{d,q}$). Fig. 5 (b) shows the average control of the three-phase system. Here, $v_{dc\_ref\_avg}$ is the expected average HV DC-link voltage for each cell unit and v_{dc_avg} is the average value of the sensed HV DC-link voltages as shown in equation (1). Here, 'n' is the total numbers of the connected cells for three phase system.

$$v_{dc\_avg} = \frac{v_{cell1} + v_{cell2} + .. + v_{celln}}{n} \qquad (1)$$

The difference between the reference and the sensed DC-link voltage is then passed through a PI control block to generate a reference d-axis current command. It is then compared with the actual i_{qd} and passed through a PI controller, which generates the compensation voltage (v_{gd}^*). Similarly, the q-axis voltage command is generated (v_{gq}^*). Equation (2) shows the detailed equation for the decoupled voltage control.

Here, v_{d_ref}, v_{q_ref} are the reference voltages generated by the decoupled controller, ω is the angular frequency and L is the grid side inductance. It is then converted to a three phase reference modulating voltages ($v_{am,bm,cm}$). These voltages are the average modulation signal which will be common for all the cell units. However, to balance individual cell units, a cell balancing control needs to be implemented, as shown in Fig. 5 (c). Here, the difference between the reference HV capacitor voltage (v_{dc_ref}) is compared with the sensed voltage from each cell (v_{dc_a,b,c_cell_m}) unit and passes through a PI controller. PI controller output is then multiplied by the unity voltage template (v_{a,b,c_unity}) to generate the compensation modulation command (v_{a,b,c_cell_m}) after adding with $v_{am,bm,cm}$. Here, m is the cell number. Whereas, in the conventional control all the cell units are loaded equally, the values of the v_{a,b,c_cell_m}, are mostly similar. The proposed control can keep the HV DC-link capacitor voltages balanced even though there is higher power imbalance between the cell units.

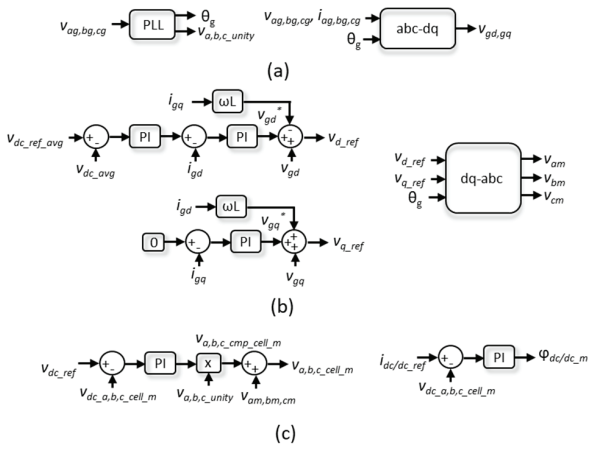

Fig. 5. Multiport EV charger control configuration; (a) PLL and dq transformation; (b) Vector control to generate three phase reference modulating voltages; (c) Cell balancing control.

$$v_{d\_ref} = v_{gd}^* + v_{gd} - i_{gq}(\omega L)$$
$$v_{q\_ref} = v_{gq}^* + v_{gq} + i_{gd}(\omega L) \qquad (2)$$

All the DC/DC converter units are tied together to serve the load power. Hence, the load current is shared in between the cell units. Here, i_{dc/dc_ref} is the current reference value for each cell unit. i_{dc/dc_cell_m} is the individual cell current. The difference between the actual and reference value is passed through a PI controller to generate the required phase shift angle.

V. SIMULATION STUDIES

Detailed simulation studies are performed to verify the control performance of the proposed system in DSIM platform. DSIM is used due to the large numbers of converter system simulation, which would not be possible to study using the conventional simulation software tools like PSIM or Matlab Simulink otherwise. Table II shows the simulated system parameters.

As shown in the table II, there are seven series connected converter units in each phase. The HV and LV side DC-link voltages are set at 1050 V and 400 V respectively. Based on the DC-link voltage, 1.7 kV IGBTs are selected for the AC/DC converter, 1.7 kV SiC for the primary side of the DC/DC converter and 1.2 kV SiC MOSFETs are used for the secondary side of the converter.

TABLE II: System Parameters

Parameter	Value
Power	350 kW
No. of cell units	21 (7 x 3)
HV DC-link voltage	1050 V
LV DC-link voltage	400 V
Grid voltage	6.6 kV

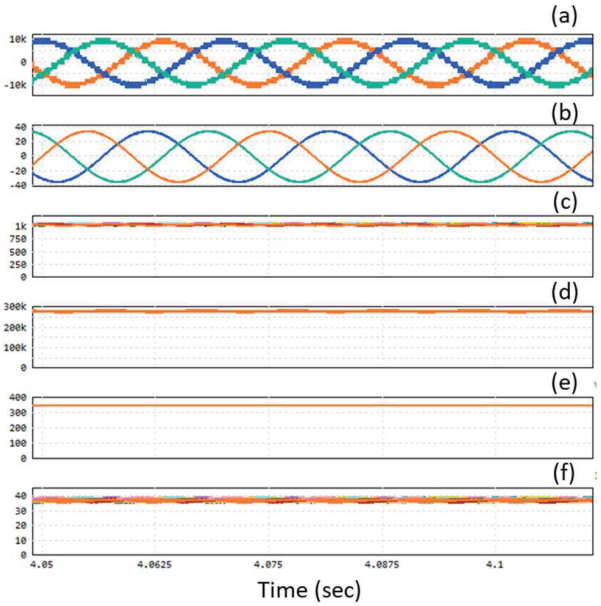

Fig. 6. Simulation results of the multiport EV charger feeding a high-power EV directly; (a) Three phase L-L voltages (V); (b) Three phase L-L currents (A); (c) A, B, C phase HV DC-link voltages; (d) Total SST output power (W); (e) LV DC-link voltage (V); (f) Individual cell output currents (A).

Fig. 6 shows the simulation results for mode I operation, where SST is feeding the charging power to the high-power EV. The other 50 kW EV chargers are not considered for this operation. As, all the cell converter output terminals are clubbed together to form a common LV DC-bus voltage, they are sharing a common DC bus voltage of 350 V and each cell will share the same load current of 38 A. The converter is feeding about 280 kW power to the charger and the proposed control can keep the HV DC-link voltages of the individual cell units balanced.

Fig. 7 shows the simulation results with the proposed power sharing strategy. Here, other than the high-power charger, which is feeding EV1, an additional lower power charger is considered which shares the same LV DC-bus with the high-power charging port. Moreover, there is another DC/DC converter used as shown in Fig. 4 (a) to interphase the variable LV DC-bus voltage with the charging terminal.

From the simulation results it can be seen that, the high-power charger (EV1) is consuming 280 kW charging power and EV2 is consuming around 6 kW. It shows the power sharing capability of the proposed system. Similarly, multiple EV charging units can also be connected at the LV DC-bus which can reroute the available erouter charging power to other EVs, with the help of additional DC/DC converters.

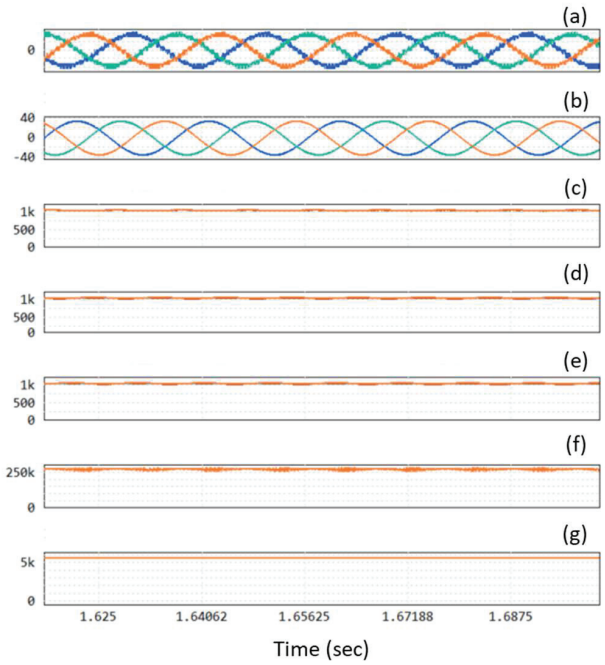

Fig. 7. Simulation results of the multiport EV charger, while charging multiple EVs simultaneously (EV1 and EV2); (a) Three phase L-L voltages (V); (b) Three phase L-L currents (A); (c, d, e) A, B, C phase HV DC-link voltages; (f) Power delivered to EV1; (g) Power delivered to EV2.

Controller could also keep the HV-DC bus voltages fixed at 1050 V for all the three phases. The grid current is sinusoidal and is in phase with the voltage, which shows the unity power factor operation of the system.

VI. EXPERIMENTAL RESULTS

Fig. 8 shows the developed 17 kW single cell unit which is used as one of the 21 cells in the developed SST converter system. Each cell is consisting of AC/DC and cascaded DC/DC converter stage. For the AC/DC converter 1.7 kV IGBT devices are used, for the DC/DC converter 1.7 kV SiC modules are used in the primary side and 1.2 kV SiC modules are used in the secondary side. The DC/DC converter is operated at 50 kHz switching frequency. The 17 kVA ferrite transformer also operates at 50 kHz and it is designed based

on 6.6 kV insulation level according to the IEC 61800-5-1 standard.

To verify the overall system control, initially one cell unit is tested in our lab. A single-phase AC voltage source is used to feed the converter and a DC electronic load is used to test the system. The AC grid voltage is measured using a voltage sensor and the sensed voltage is feed back to the ADC port of the controller unit. All the interphase with the central controller and the individual control board is done using a fiber optics cable. For individual cell control FPGA controller XC6SLX9-2TQG144C (SPARTAN-6) is used. All the protection and PWM switching is done using this controller boards mounted on the 21 cell units. The overall system control is implemented using PE-Expert 4 controller.

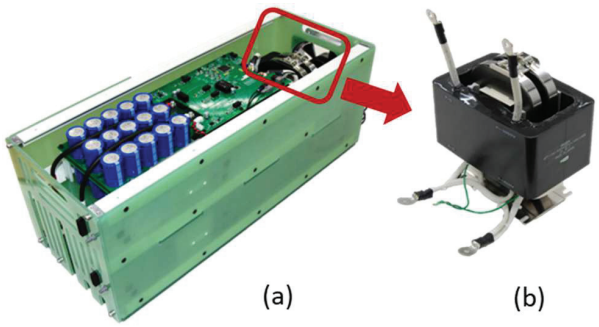

Fig. 8. Developed 17 kW cell unit (AC/DC/DC); (a) One cell unit; (b) 50 kHz high frequency (HF) transformer.

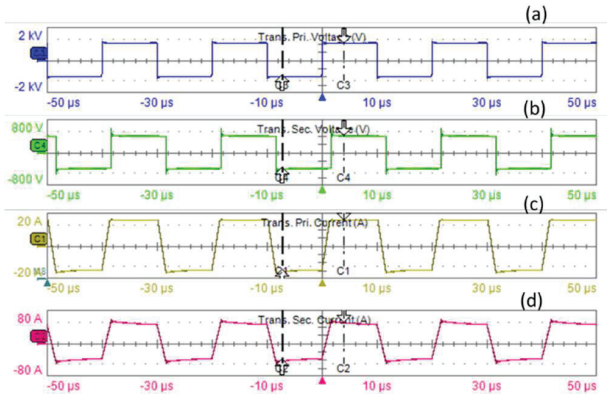

Fig. 9. Experimental results of a 17 kW DC/DC converter; (a) Primary side transformer voltage (V); (b) Secondary side transformer voltage (V); (c) Primary side transformer current (A); (d) Secondary side transformer current (A).

Fig. 9 shows the experimental results of the DC/DC converter with 50 kHz switching frequency and 17 kW load. The primary side voltage of the DC/DC converter is 1050 V and the secondary side load voltage is 392 V. The primary and secondary side peak currents are 15 A and 45 A respectively.

VII. CONCLUSIONS

A multiport 350 kW 6.6 kV EV charger is proposed with a reduced overall footprint area and cost. The proposed system can directly charge a high-power EV from the SST converter without any intermediate DC/DC converter stage. The SST converter available power can also be shared with other lower power EV charging ports with the help of additional isolated DC/DC converters. Compared to the conventional SST based EV charger, in the proposed configuration the LV DC-bus voltage is variable. Detailed simulation study is presented to demonstrate the performance of the proposed system. A 17-kW prototype is also developed and tested to check the system performance for a single cell unit.

References

[1] S. Srdic and S. Lukic, "Toward extreme fast charging: challenges and opportunities in directly connecting to medium-voltage line," *IEEE Electrif. Magazine*, vol. 7, no.1, pp. 22– 31, Mar. 2019.

[2] X. She, A. Q. Huang, T. Zhao, and G. Wang, "Coupling effect reduction of a voltage-balancing controller in single-phase cascaded multilevel converters," *IEEE Trans. Power Electron.*, vol. 27, no.87, pp. 3530– 3543, Aug. 2012.

[3] J. Liu, J. Yang, J. Zhang, Z. Nan, and Q. Zheng, "Voltage balance control based on dual active bridge DC/DC converters in a power electronic traction transformer," *IEEE Trans. Power Electron.,* vol. 33, no. 2, pp. 1696-1714, Feb. 2018.

[4] A. D. Aquila, M. Liserre, V. G. Monopoli, and P. Rotondo, "Overview of PI-based solutions for the control of DC buses of a single-phase H-bridge multilevel active rectifier," *IEEE Trans. on Ind. Appl.* vol. 44, no. 3, pp. 857-866, May/June 2008.

[5] J. Miao, N. Zhang, C. Kang, J. Wang, Y. Wang, and Q. Xia, "Steady-state power flow model of energy router embedded AC network and its application in optimizing power system operation," *IEEE Trans. Smart Grid,* vol. 9, no. 5, pp. 4828-4837, Sept. 2018.

[6] X. She, A. Q. Huang, and G. Wang, "3-D space modulation with voltage balancing capability for a cascaded seven-level converter in a solid-state transformer," *IEEE Trans. Power Electron.*, vol. 26, no. 12, pp. 3778– 3789, Dec. 2011.

[7] C. Zhu, "High-efficiency, medium-voltage input, solid-state, transformer based 400 kW/ 1000 V/400 A extreme fast charger forelectricvehicle,"Link:https://www.energy.gov/sites/default/files/2021-06/elt241_zhu_2021_o_5-24_126pm_LR_TM.pdf.

[8] V. M. Iyer, S. Gulur, G. Gohil, and S. Bhattacharya, "An approach towards extreme fast charging station power delivery for electric vehicles with partial power processing," *IEEE Trans. Ind. Electron.*, vol. 67, no. 10, pp. 8076–8087, Oct. 2020.

[9] A. C. Nair, and B. G. Fernandes, "A solid state transformer based fast charging station for various categories of electric vehicles with battery of vastly different ratings," *IEEE Trans. Indus. Electron.*, vol. 68, no. 11, pp. 10400–10411, Oct. 2021.

[10] E. I. Pool-Mazun, J. J. Sandoval, P. N. Enjeti, and I. J. Pital, "An integrated solid-state transformer with high-frequency isolation for EV fast-charging applications," *IEEE J. of Emg. and Selec. Topics in Ind. Electron.,* vol. 1, no. 1, pp. 46–56, July 2020.

[11] G. J. Pierre, S. Beheshtaein, N. Altin, and A. Nasiri, "Control and loss analysis of a solid-state transformer-based DC extreme fast charger," in *proc. IEEE Trans. Electrification Conf. and Expo.*, 2021, pp. 1-6.

[12] A. Choudhury, Y. Mabuchi, and K. Furukawa, "High voltage side DC-bus capacitor voltage balancing control of a 350-kW multiport EV charging system," in *proc. IEEE Energy conver. Congr. and Expo.* (ECCE), Oct. 2022, pp. 1-6.